

## QUASI MODES AND DENSITY OF STATES (DOS) OF 1D PHOTONICS CRYSTAL

Shaolin Liao<sup>1,\*</sup> and Lu Ou<sup>2</sup>

<sup>1</sup> (2008-2010) Physics Department, Queens College, City University of New York, 65-30 Kissena Blvd, Flushing NY 11367;

<sup>2</sup> College of Computer Science and Electronic Engineering, Hunan University, Changsha, Hunan, China 410082.

\*Corresponding author (sliao5@iit.edu): S. Liao is now at the Department of Electrical and Computer Engineering, Illinois Institute of Technology, Chicago, IL, USA 60616.

**Abstract**—1-Dimensional (1D) photonics crystals with and without defects have been numerically studied using efficient Transfer Matrix Method (TMM). Detailed numerical recipe of the TMM has been laid out. Dispersion relation is verified for the periodic Photonics Band Gap (PBG) structure. When there are defects, the transmission spectrum can be decomposed into one or more quasi modes with excellent agreement. The Density of States (DOS) is obtained from the phase derivative of the transmission spectrum. Green's function is also obtained showing much sharper mode characteristics when the excitation source is localized at the peaks of the quasi modes.

### 1. INTRODUCTION

Photonics crystal has been of great interest due to its potential applications in optics filter and low-loss reflection mirror [1], [2]. The transmission spectrum and its phase information of different kinds of photonics crystal has been widely reported using Transfer Matrix Method (TMM) [2]. Experiment on single-mode 1-dimensional (1D) waveguide system has been recently carried out in our group [3]. What's more, the Green's function is important in description of random laser [4] and periodic Photonics Band Gap (PBG) structure with defects [3] since the radiation can be understood as convolution of the Green's function with the source. Also, Local Density of States (LDOS) is closely related to the imaginary part of the Green's function [5]. The Density of States (DOS), which is the volume integral of the

LDOS, is shown to be the phase derivative of the transmission spectrum with respect to frequency for 1D system without loss [6].

In this article, we numerically study the transmission spectrum, its phase information and the Green's function, by means of TMM [2]. The obtained 1D transmission spectrum is further decomposed into quasi modes [7]. The DOS is obtained from the phase derivative of the transmission spectrum.

## 2. TRANSFER MATRIX METHOD

The electromagnetic wave is governed by the Maxwell's equations and has many applications [8]-[70]. Here we are dealing with the 1D problem in the optics regime.

### 2.1. Green's function

The Green's function is described by

$$\nabla^2 G(x, x') + k^2(x)G(x, x') = -\delta(x - x') \quad (1)$$

where the delta source is located at  $x'$ .

The boundary conditions are

$$\begin{aligned} G(x_b^+, x') &= G(x_b^-, x') \\ \frac{dG(x_b^+, x')}{dx} - \frac{dG(x_b^-, x')}{dx} &= -\delta(x_b - x') \end{aligned} \quad (2)$$

where  $x_b^\pm$  denote the right and left sides of the boundary.

### 2.2. Forward- and backward- propagating waves

The Green's function  $G(x, x')$  in each layer can be expressed as superposition of forward- and back-ward propagating waves,

$$G(x, x') = t \exp^{-jk_0(n_r - jn_i)x} + r \exp^{jk_0(n_r - jn_i)x} \quad (3)$$

where  $n_r - jn_i$  is the complex index of refractive.

#### 2.2.1. On the layer boundary

Substituting Eq. (3) into Eq. (2) and setting  $x_b = 0$ , we have,

$$\underline{v}^\pm = T^\pm \underline{v}^\mp + S^\pm \underline{u} \quad (4)$$

where the superscript ”+” denotes the right side of the boundary and ”-” denotes the left side of the boundary. The transfer matrixes  $T^\pm$  and source matrixes  $S^\pm$  are given below,

$$T^\pm = \frac{1}{2} \begin{bmatrix} 1 + \frac{n_r^\mp - jn_i^\mp}{n_r^\pm - jn_i^\pm} & 1 - \frac{n_r^\mp - jn_i^\mp}{n_r^\pm - jn_i^\pm} \\ 1 - \frac{n_r^\mp - jn_i^\mp}{n_r^\pm - jn_i^\pm} & 1 + \frac{n_r^\mp - jn_i^\mp}{n_r^\pm - jn_i^\pm} \end{bmatrix}$$

$$S^\pm = \pm \frac{1}{2} \begin{bmatrix} 1 & \frac{1}{n_r^\pm - jn_i^\pm} \\ 1 & \frac{-1}{n_r^\pm - jn_i^\pm} \end{bmatrix}$$

### 2.2.2. Wave propagations inside layer

The wave propagations inside each layer can be described by a propagators  $P^\pm$ ,

$$\underline{v}_m^\pm = P_m^\pm \underline{v}_m^\mp \quad (5)$$

where  $\pm$  denote the left and right ends of layer  $m$  respectively, and

$$P_m^\pm = \begin{bmatrix} \exp^\mp jk_0(n_r^m - jn_i^m)d_m & 0 \\ 0 & \exp^\pm jk_0(n_r^m - jn_i^m)d_m \end{bmatrix}$$

where  $d_m$  is the thickness of layer  $m$ .

### 2.2.3. The excitation source

From Eq. (4), we know that, away from the source location  $x'$ ,

$$\underline{v}^\pm = T^\pm \underline{v}^\mp \quad (6)$$

At the excitation source location, we have

$$\underline{v}^+ = \underline{v}^- + \begin{bmatrix} \frac{-j}{2k_0} \frac{1}{n_r - jn_i} \\ \frac{j}{2k_0} \frac{1}{n_r - jn_i} \end{bmatrix} \quad (7)$$

where  $n_r - jn_i$  is complex index of refractive at the source location  $x'$ .

## 2.3. Numerical recipe

The numerical recipe to obtain the 1D Green's function is as follows, 1) individually, calculate the transmission and reflection spectra for the segments to the left and to the right sides of the source location  $x'$ , through Eq. (5) and Eq. (6); 2) connect both segments at the source location, through Eq. (7).

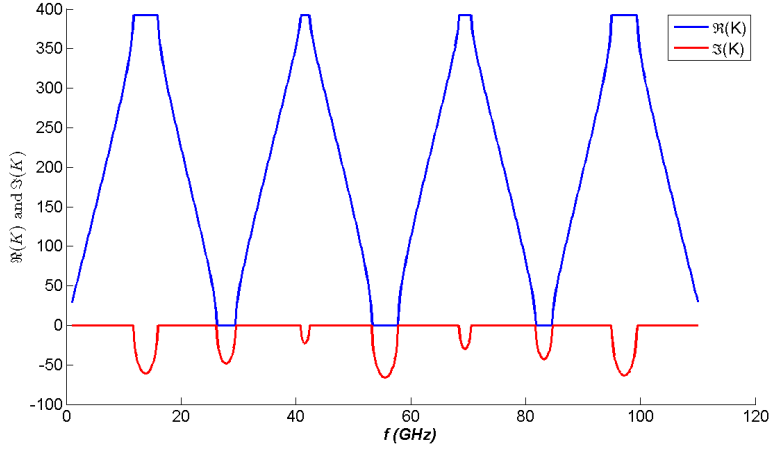


**Figure 1.** Dispersion relation of a typical PBG structure:  $a = 2d_1 = 2d_2 = 8$  mm;  $n_1 = 1$  and  $n_2 = 1.7$ .

### 2.3.1. The left and right segments

For each segment, we have to cascade the propagator  $P^-$  in Eq. (5) and the transfer matrix  $T^-$  in Eq. (6), i.e., the cascading procedure has to be done from the end of each segment, where there is only forward propagating wave,

$$\underline{v}^+(\text{left/right}) = \left[ \prod_{m=1}^N P_m^- T_m^- \right] \begin{bmatrix} 1 \\ 0 \end{bmatrix} \quad (8)$$

### 2.3.2. Connect both segments

We now connect both segments at the source location through Eq. (7),

$$\begin{aligned} t(\text{right}) &= t(\text{left}) - \frac{j}{2k_0} \frac{1}{n_r - jn_i} \\ r(\text{right}) &= r(\text{left}) + \frac{j}{2k_0} \frac{1}{n_r - jn_i} \end{aligned} \quad (9)$$

### 3. PERIODIC PBG STRUCTURE

It is well-known that the dispersion relation of the periodic binary dielectric layers is given by [71],

$$\cos(Ka) = \cos(k_1d_1) \cos(k_2d_2) - \frac{k_1^2 + k_2^2}{2k_1k_2} \sin(k_1d_1) \sin(k_2d_2) \quad (10)$$

where  $K$  is the wave vector of the Bloch wave;  $k_{1,2} = \omega\sqrt{\mu\epsilon_{1,2}}$  are the wave vector of the binary pair;  $a = d_1 + d_2$  is the periodicity of the structure, with  $d_{1,2}$  being the thickness of each layer. Fig. 1 shows a typical dispersion relation for  $a = 2d_1 = 2d_2 = 8$  mm;  $n_1 = 1$  and  $n_2 = 1.7$ ; the frequency ranges from 1 GHz to 110 GHz. The simulated transmission spectrum for such periodic PBG structure has been carried out for 25 pairs of binary dielectric layers: incident wave from left and transmitted wave on the right. The result is shown in Fig. 2, which agrees well with Fig. 1.

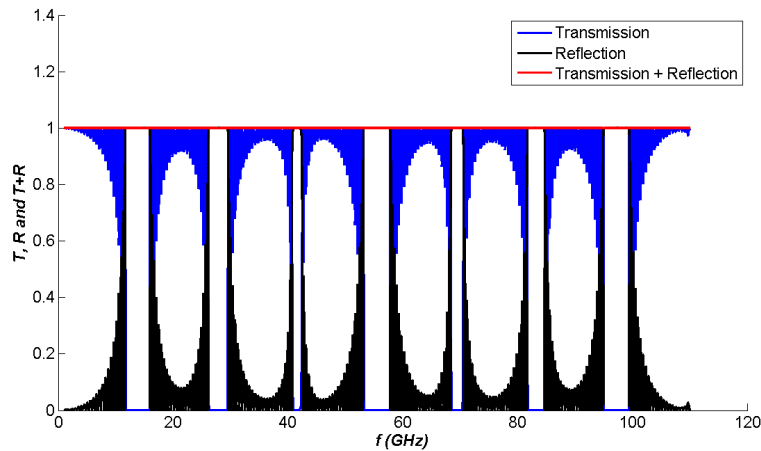


**Figure 2.** Transmission intensity  $T$ , reflection intensity  $R$  and their sum  $T + R$  for 25 pairs of dielectric layers.

## 4. DEFECTS AND QUASI MODES

### 4.1. Transmission and reflection spectra

Now let's look at what happens when one or more defects are introduced deep inside the PBG structure (25 pairs). First, let's look

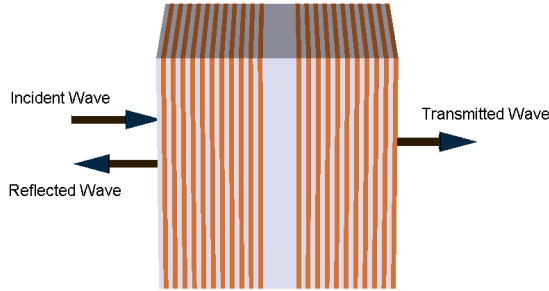


**Figure 3.** Single defect inside PBG structure is simulated: 3 pairs in the middle are replaced with  $n_1$ . Gray:  $n_1 = 1$ ; Orange:  $n_2 = 1.7$ .

at single potential well (defect) by replacing the middle 3 pairs with  $n_1$  (see Fig. 3). The result is shown in Fig. 4 for the first band gap in Fig. 2. One quasi modes appears at around  $f_c = 14.85$  GHz. A closer look at the intensity and phase of the transmission and reflection spectrum are shown in Fig. 5 and Fig. 6, together with the quasi mode fitting and DOS. Quasi modes will be explained in Section 4.2 and DOS is discussed in Section 4.3.

Now let's look at double potential wells (defects) by replacing 3 pairs with  $n_1$  (see Fig. 7) at two locations separated by a potential barrier  $n_2$ . The intensity and phase are shown in Fig. 8 and Fig. 9 respectively. Also see Section 4.2 for quasi mode explanation and Section 4.3 for DOS.

## 4.2. Quasi modes

Quasi modes can be considered as localized modes around the defect sites and could couple with each other if more than one modes are present. Mathematically, the frequency part of the quasi mode can be expressed as the Lorentzian function,

$$\Psi(f) = \frac{\Gamma}{(f - f_c) + j\Gamma} \quad (11)$$

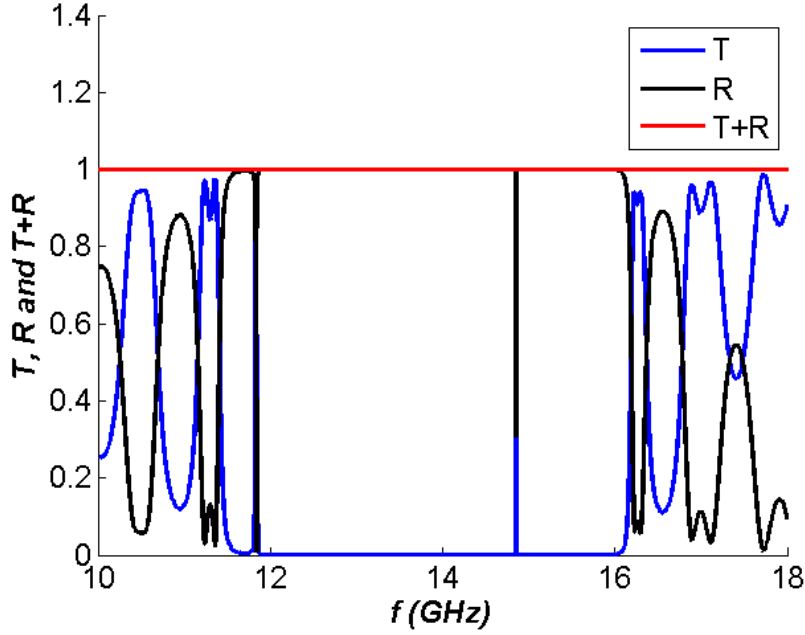


**Figure 4.** First band gap of PBG structure with single defect: transmission intensity  $T$ , reflection intensity  $R$  and their sum  $T + R$ .

#### 4.2.1. Single quasi mode

In Fig. 5 and Fig. 6, we look closer into the quasi mode shown in Fig. 4. We also plot the Lorentzian quasi mode as circles in Fig. 5 and Fig. 6, which agrees with the simulation very well. We found that  $f_c = 14.85$  GHz and  $\Gamma = 0.131$  MHz for this quasi mode.

#### 4.2.2. Two quasi modes

For double defects inside PBG structure., the wave function can be expressed in sum of two quasi modes,

$$\Psi(f) = a_1 \frac{\Gamma_1}{(f - f_1) + j\Gamma_1} + a_2 \exp^{j\pi} \frac{\Gamma_2}{(f - f_2) + j\Gamma_2} \quad (12)$$

with  $f_1 = 14.810$  GHz,  $\Gamma_1 = 4.5$  MHz,  $a_1 = 0.972$  and  $f_2 = 14.898$  GHz,  $\Gamma_2 = 5.1$  MHz,  $a_2 = 0.966$ . Note that in Eq. (12), the phase difference between these adjacent two modes is  $\pi$ .

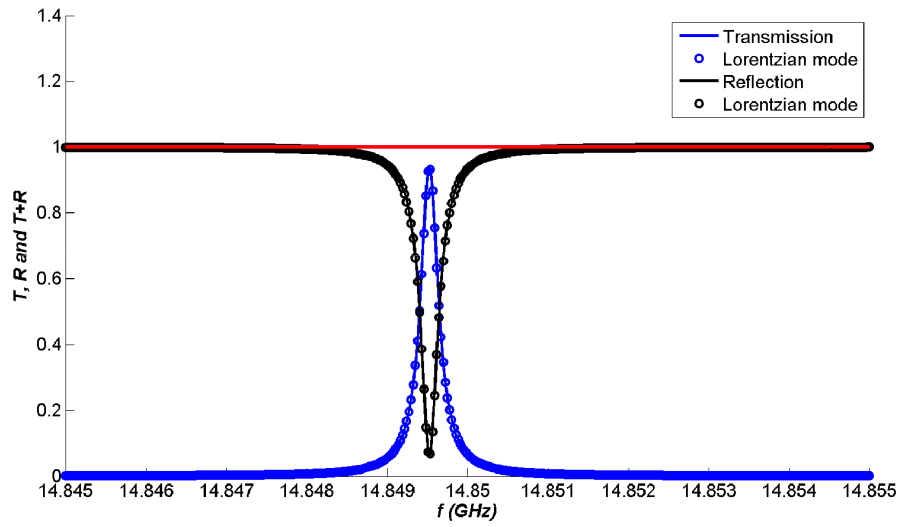


**Figure 5.** Single defect (a closer look of Fig. 4): simulated intensity and that of the theoretical Lorentzian quasi mode, with  $f_c = 14.85$  GHz and  $\Gamma = 0.131$  MHz.

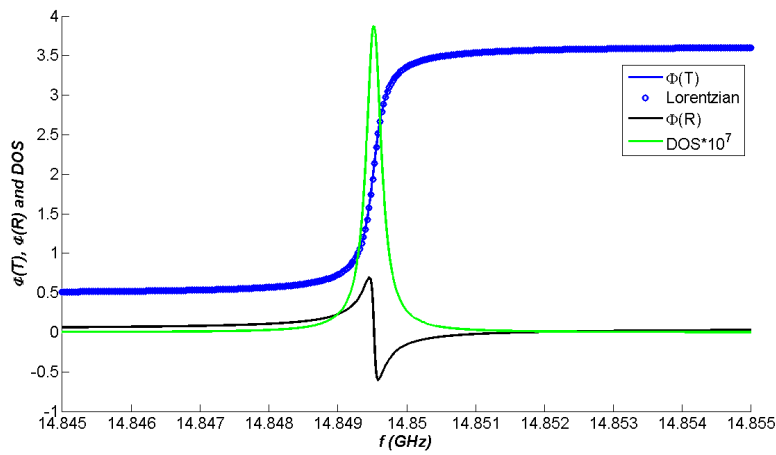


**Figure 6.** Single defect: simulated phase and and that of the Lorentzian quasi mode, with  $f_c = 14.85$  GHz and  $\Gamma = 0.131$  MHz.



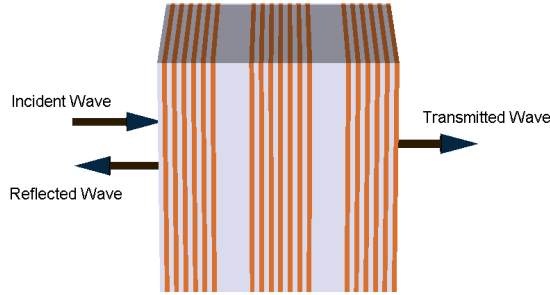


**Figure 7.** Double defects inside PBG structure is simulated: 3 pairs at two locations are replaced with  $n_1$ , separating by a potential barrier  $n_2$ . Gray:  $n_1 = 1$ ; Orange:  $n_2 = 1.7$ .

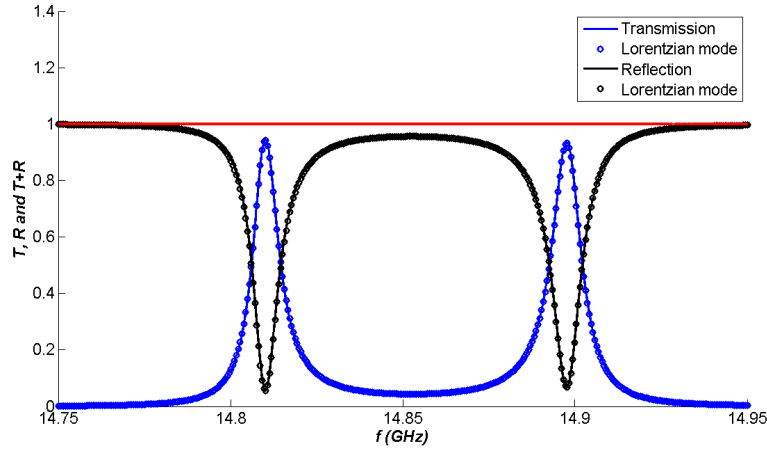


**Figure 8.** Double defects: simulated transmission and reflection intensities and those of the sum of two Lorentzian quasi modes, with  $f_1 = 14.810$  GHz,  $\Gamma_1 = 4.5$  MHz and  $f_2 = 14.898$  GHz,  $\Gamma_2 = 5.1$  MHz.

### 4.3. Density of States

For 1D system, DOS is given by [6],

$$\text{DOS} = \frac{1}{\pi} \frac{d\phi}{d\omega} \quad (13)$$

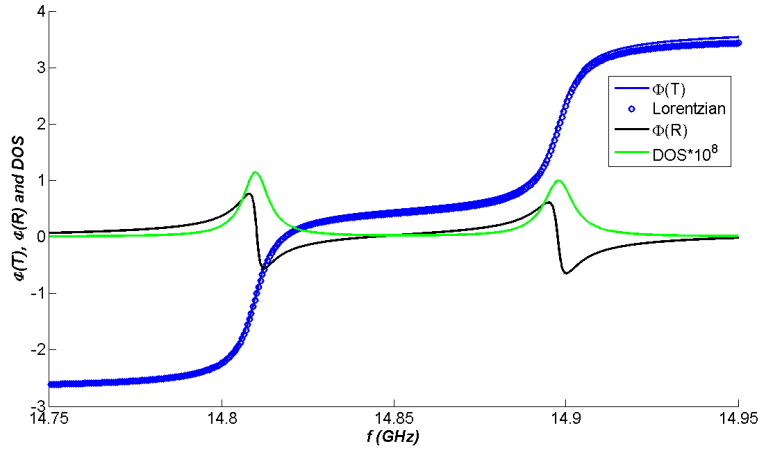


**Figure 9.** Double defects: simulated phase and that of the sum of two Lorentzian quasi modes, with  $f_1 = 14.810$  GHz,  $\Gamma_1 = 4.5$  MHz and  $f_2 = 14.898$  GHz,  $\Gamma_2 = 5.1$  MHz.

We also plot the DOS for single defect and double defects in Fig. 6 and Fig. 9 respectively.

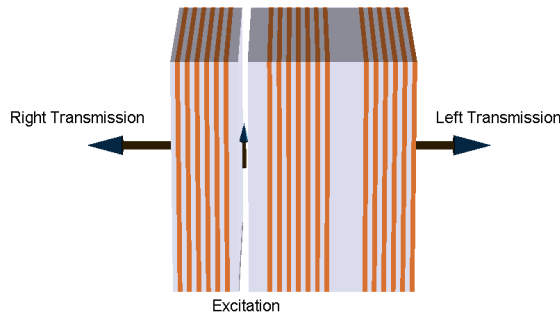


**Figure 10.** Schematics of Green's function for double defects. Gray:  $n_1 = 1$ ; Orange:  $n_2 = 1.7$ .

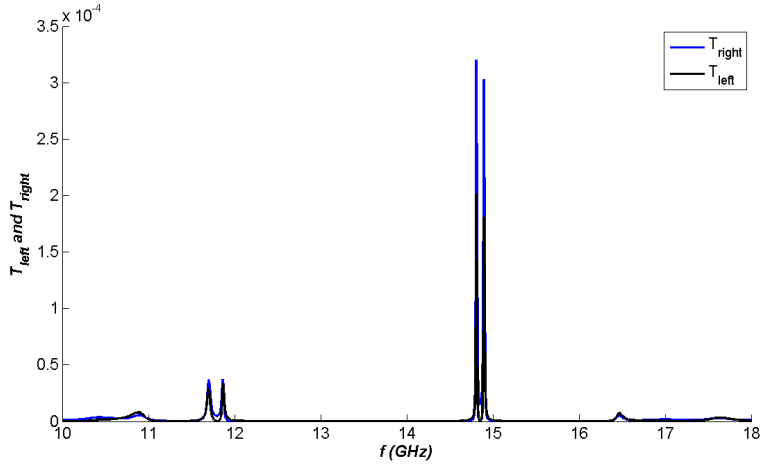


**Figure 11.** Simulated transmission spectrum of Green's function for both left and right transmissions.

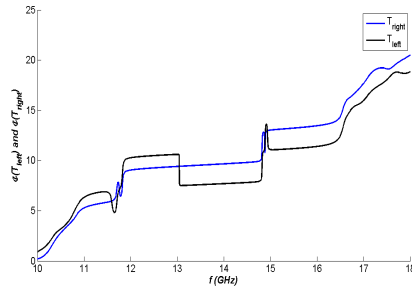


**Figure 12.** Simulated phase of the transmission spectrum of Green's function for both left and right transmissions.

#### 4.4. Green's function

We also obtained the Green's function following the procedure stated in Section 2.3. Here we show the result for double defects: the schematics with excitation source inside the first defect is shown in Fig. 10. The transmission spectra and phases for both left and right sides are shown in Fig. 11 and Fig. 12 respectively. Compared to the transmission and reflection spectra in Fig. 8 and Fig. 9, we can see that the Green's function shows much sharper quasi mode peaks.

## 5. CONCLUSION

We have simulated the transmission spectrum and the Green's function for 1D photonics crystal with and without defects. It has been shown that quasi mode decomposition gives excellent agreement with the simulated result. DOS is also obtained through the phase derivative of the transmission spectrum. The method can find applications in design of 1D photonics filter and reflection mirror, defect simulation of photonics crystal and its DOS.

## ACKNOWLEDGMENT

Shaolin Liao wants to thank Prof. Azriel Genack and his group for their help when he worked there as a Postdoc Fellow from 2008-2010.

## REFERENCES

1. Yablonovich, E., "Inhibited spontaneous emission in solid-state physics and electronics," *Phys. Rev. Lett.* , Vol. 58, 2059, 1987.
2. Wu, C. J., Chu, B. H., Weng M. D., and Lee, H. L., "Enhancement of bandwidth in a chirped quarter-wave dielectric mirror," *J. Electromagn. Waves and Appl.* , Vol. 23, No. 4, 437-447, 2009.
3. Sebbah, P., Hu, B., Klosner, J., and Genack, Z. A., "Quasimodes of spatially extended field distributions within nominally localized random waveguides," *Phys. Rev. Lett.* , 96, 183902, 2006.
4. Tureci H. E., Douglas, S. A., and Collier, B., "Self-consistent multimode lasing theory for complex or random lasing media," *Physical Review A* , Vol. 74, 043822, 2006.
5. Sheng, P., *Introduction to Wave Scattering, Localization and Mesoscopic Phenomena* , second edition, Springer, 2006.
6. Avishai, Y. and Band, Y. B., "One-dimensional density of states and the phase of the transmission amplitude," *Rapid Communications, Physical Review B* , Vol. 32, No. 4, August, 1985.
7. Ching, E. S. C., Leung, P. T., Maassen, A., Suen, W. M., Tong, S. S., and Young K., "Quasinormal-mode expansion for waves in open systems," *Reviews of Modern Physics* , Vol. 70, No. 4, October 1998.
8. S. Liao and L. Ou, A Ping-Pong Computational Electromagnetics (CEM) Algorithm for 2D Antennas/Metasurfaces, *2020 Asia-Pacific Microwave Conference (APMC 2020)*, Hong Kong SAR, PR China, 8-11 December, 2020. Also available at arXiv.

9. S. Liao and L. Ou, Iterative Physical Optics (IPO) for Fast and Accurate Simulation of Reflector Antennas, *2020 Asia-Pacific Microwave Conference (APMC 2020)*, Hong Kong SAR, PR China, 8-11 December, 2020. arXiv:2007.01861: <https://arxiv.org/abs/2007.01861>
10. S. Liao and L. Ou, Ultra-sensitive Parity-Time Symmetry based Graphene FET (PTS-GFET) Sensors, *2020 Asia-Pacific Microwave Conference (APMC 2020)*, Hong Kong SAR, PR China, 8-11 December, 2020. arXiv:2007.04567: <https://arxiv.org/abs/2007.04567>
11. S. Liao, T. Elmer, S. Bakhtiari, N. Gopalsami, N. Cox, J. Wiencek, A. C. Raptis, "Standoff Through-the-Wall Sensing at Ka-Band Microwave," Materials Evaluation, American Society of Nondestructive Testing, vol. 70, no. 10, pp. 1136-1145, Oct. 2012. Also available at arXiv:2007.06020, <https://arxiv.org/abs/2007.06020>.
12. Sanchith Padmaraj K. Nirish Patil and S. Liao, A Compact Dual-band WiFi Energy Harvester, *2019 Photonics & Electromagnetics Research Symposium - Fall (PIERS - Fall)*, Xiamen, China, 2019, pp. 1209-1212. DOI: 10.1109/PIERS-Fall48861.2019.9021903
13. Y. He Y. Li Z. Zhou H. Li Y. Hou S. Liao and P. Chen, Wideband Epsilon-Near-Zero Supercoupling Control through Substrate-Integrated Impedance Surface, *Advanced Theory and Simulations*, vol. 2, no. 8, p. 1900059, 2019, DOI: 10.1002/adts.201900059.
14. S. Liao and L. Ou, "iESC: iterative Equivalent Surface Current Approximation," available at <https://arxiv.org>, July 2020.
15. S. Liao, Multi-frequency beam-shaping mirror system design for high-power gyrotrons: Theory, algorithms and methods, *ProQuest Dissertations And Theses; Thesis (Ph.D.)The University of Wisconsin - Madison*, 2008.; Publication Number: AAI3314260; ISBN: 9780549633167; Source: Dissertation Abstracts International, Volume: 69-05, Section: B, pp. 1-245. <https://ui.adsabs.harvard.edu/abs/2008PhDT.....81L/abstract> or <https://dl.acm.org/doi/book/10.5555/1467404>
16. L. Ou, S. Liao, Z. Qin, and H. Yin, Millimeter Wave Wireless Hadamard Image Transmission for MIMO enabled 5G and Beyond, *IEEE Wireless Communications*, pp. 1536-1284, 2020. DOI: 10.1109/MWC.001.2000081
17. S. Liao, Z. Wang, L. Ou, and Y. Peng, A Harmonics Interferometric Doppler Sensor With a Neon Lamp Detector, *IEEE Sensors Journal*, pp. 1-1, 2020, DOI: 10.1109/JSEN.2020.2970055.
18. S. Liao, N. Gopalsami, S. Bakhtiari, T. W. Elmer, E. R. Koehl, and A. C. Raptis, A novel interferometric sub-THz Doppler radar

- with a continuously oscillating reference arm, *IEEE Transactions on Terahertz Science and Technology*, vol. 4, no. 3, pp. 307-313, Mar. 2014. DOI: 10.1109/TTHZ.2014.2307165
19. S. Liao et al., Passive millimeter-wave dual-polarization imagers, *IEEE Transactions on Instrumentation and Measurement*, vol. 61, no. 7, pp. 2042 - 2050, Feb. 2012. DOI: 10.1109/TIM.2012.2183032
  20. N. Gopalsami, S. Liao, T. Elmer, E. Koehl, A. Heifetz, A. Raptis, L. Spinoulas, and A. Katsaggelos, Passive millimeter-wave imaging with compressive sensing, *Optical Engineering*, vol. 51, no. 9, pp. 091614-1:9, Sep. 2012. DOI: 10.1117/1.OE.51.9.091614
  21. S. Bakhtiari, T. Elmer, M. Cox, N. Gopalsami, A. Raptis, S. Liao, I. Mikhelson and A. Sahakian, Compact Millimeter-Wave Sensor for Remote Monitoring of Vital Signs, *IEEE Transactions on Instrumentation and Measurement*, vol. 61, no. 3, pp. 830-841, Mar. 2012, DOI: 10.1109/TIM.2011.2171589.
  22. S. Liao, N. Gopalsami, A. Venugopal, A. Heifetz, and A. C. Raptis, An efficient iterative algorithm for computation of scattering from dielectric objects, *Optics Express*, vol. 19, no. 3, pp. 3304-3315, 2011. DOI: 10.1364/OE.19.003304
  23. S. Bakhtiari, S. Liao, T. Elmer, N. Gopalsami, and A. C. Raptis, A real-time heart rate analysis for a remote millimeter wave I-Q sensor, *IEEE Transactions on Biomedical Engineering*, vol. 58, no. 6, pp. 1839-45, Mar. 2011. DOI: 10.1109/TBME.2011.2122335
  24. A. Heifetz, H. T. Chien, S. Liao, N. Gopalsami, and A. C. Raptis, Millimeter-wave scattering from neutral and charged water droplets, *Journal of Quantitative Spectroscopy and Radiative Transfer*, vol. 111, no. 17-18, pp. 2550-2557, 2010. DOI: 10.1016/j.jqsrt.2010.08.001
  25. S. Liao and R. J. Vernon, A fast algorithm for computation of electromagnetic wave propagation in half-space, *IEEE Trans. on Antennas and Propagation*, vol. 57, no. 7, pp. 2068-2075, Jul. 2009. DOI: 10.1109/TAP.2009.2021890
  26. S. Liao, Miter bend mirror design for corrugated waveguides, *Letters of Progress in Electromagnetics Research*, vol. 10, pp. 157-162, 2009. DOI: 10.2528/PIERL09062103
  27. S. Liao and R. J. Vernon, Sub-THz beam-shaping mirror designs for quasi-optical mode converter in high-power gyrotrons, *Journal of Electromagnetic Waves and Applications*, vol. 21, no. 4, pp. 425-439, 2007. DOI: 10.1163/156939307779367332
  28. S. Liao and R. J. Vernon, A fast algorithm for wave propagation from a plane or a cylindrical surface, *International Journal of Infrared and Millimeter Wave*, vol. 28, no. 6, pp. 479-490, 2007.

DOI: 10.1007/s10762-007-9213-0

29. S. Liao, The Taylor Interpolation through FFT Algorithm for Electromagnetic Wave Propagation and Scattering, *arXiv:physics/0610057*, Oct. 2006. <https://arxiv.org/abs/physics/0610057>
30. S. Liao and L. Ou, High-speed Millimeter-wave 5G/6G Image Transmission via Artificial Intelligence, *2020 Asia-Pacific Microwave Conference (APMC 2020)*, Hong Kong SAR, PR China, 8-11 December, 2020. arXiv:2007.03153: <https://arxiv.org/abs/2007.03153>
31. I. V. Mikhelson, S. Bakhtiari, T. W. E. II, S. Liao, and A. V. Sahakian, Remote sensing of heart rate using millimeter-wave interferometry and probabilistic interpolation, in *Proceedings SPIE 8719, Smart Biomedical and Physiological Sensor Technology X*, 2013, vol. 8719M. DOI: 10.1117/12.2015282
32. S. Liao, N. Gopalsami, S. Bakhtiari, T. Elmer, and A. C. Raptis, A novel interferometric millimeter wave Doppler radar, *2013 IEEE International Instrumentation and Measurement Technology Conference (I2MTC)*, Minneapolis, MN, 2013, pp. 387-391. DOI: 10.1109/I2MTC.2013.6555445
33. S. Liao et al., Millimeter Wave Doppler Sensor for Nondestructive Evaluation of Materials, *21st Annual Research Symposium & Spring Conference 2012*, Dallas, TX USA, 2012. arXiv:2007.00195: <https://arxiv.org/abs/2007.00195>
34. S. Liao, S. Bakhtiari, T. Elmer, A. C. Raptis, I. V. Mikhelson, and A. V. Sahakian, Millimeter wave I-Q standoff biosensor, in *Proceedings SPIE 8371, Sensing Technologies for Global Health, Military Medicine, Disaster Response, and Environmental Monitoring II; and Biometric Technology for Human Identification IX*, 2012, vol. 8371D. DOI: 10.1117/12.924241
35. N. Gopalsami, S. Liao, T. Elmer, E. R. Koehl, and A. C. Raptis, Evaluation of passive millimeter wave system performance in adverse weather, in *Proceedings SPIE 8362, Passive and Active Millimeter Wave Imaging XV, 2012*, vol. 8362O. DOI: 10.1117/12.919212
36. N. Gopalsami, T. W. Elmer, S. Liao, R. Ahern, A. Heifetz, A. C. Raptis, M. Luessi, D. Babacan and A. K. Katsaggelos, Compressive sampling in passive millimeter wave imaging, in *Proceedings of SPIE 8022, Passive Millimeter-Wave Imaging Technology XIV*, 2011, vol. 8022O. DOI: 10.1117/12.886998
37. N. Gopalsami, S. Liao, T. Elmer, A. Heifetz and A. C. Raptis, Compressive sampling in active and passive millimeter-wave

- imaging, *2011 International Conference on Infrared, Millimeter, and Terahertz Waves*, Houston, TX, 2011, pp. 1-2. DOI: 10.1109/IRMMW-THz.2011.6105205
38. E. Buscarino, S. Liao, M. Perkins, B. Rock, U. Farid and R. Vernon, High-Power Microwave Transmission and Mode Conversion Program, Report to USA DOE Office, 2005, DOI: 10.2172/1210042
  39. S. Liao, Validity of image theorem under spherical geometry, *Progress in Electromagnetics Research Symposium (PIERS)*, Marrakesh, Morocco, 2011. arXiv:2007.02000: <https://arxiv.org/abs/2007.02000>
  40. S. D. Babacan, M. Luessi, L. Spinoulas, A. K. Katsaggelos, N. Gopalsami, T. Elmer, R. Ahern, S. Liao and A. Raptis, Compressive passive millimeter-wave imaging, *2011 18th IEEE International Conference on Image Processing*, Brussels, 2011, pp. 2705-2708. DOI: 10.1109/ICIP.2011.6116227
  41. N. Gopalsami, S. Liao, E. R. Koehl, T. W. Elmer, A. Heifetz, H.-T. Chien and A. C. Raptis, Passive millimeter wave imaging and spectroscopy system for terrestrial remote sensing, in *Proceedings of SPIE 7670, Passive Millimeter-Wave Imaging Technology XIII*, 2010, vol. 767003. DOI:10.1117/12.850123
  42. R. J. Vernon, S. Liao and J. Neilson, A high-efficiency four-frequency mode converter design with small output angle variation for a step-tunable gyrotron, in *2008 33rd International Conference on Infrared, Millimeter and Terahertz Waves*, Pasadena, CA, USA, 2008. DOI: 10.1109/ICIMW.2008.4665569
  43. S. Liao, Vernon RJ and Neilson J., A four-frequency mode converter with small output angle variation for a step-tunable gyrotron, *Proceedings of the 15th Joint Workshop On Electron Cyclotron Emission and Electron Cyclotron Resonance Heating, EC-15*. 477-482, 2009. DOI: 10.1142/9789812814647\_0068
  44. S. Liao, On the validity of physical optics for narrow-band beam scattering and diffraction from the open cylindrical surface, *Progress in Electromagnetics Research Symposium (PIERS)*, vol. 3, no. 2, pp. 158-162, 2007. DOI:10.2529/PIERS060906142312
  45. S. Liao, Fast computation of electromagnetic wave propagation and scattering for quasi-cylindrical geometry, *Progress in Electromagnetics Research Symposium (PIERS)*, vol. 3, no. 1, pp. 96-100, 2007. DOI:10.2529/PIERS060906005903
  46. S. Liao, Beam-shaping PEC mirror phase corrector design, *Progress in Electromagnetics Research Symposium (PIERS)*, vol. 3, no. 4, pp. 392-396, 2007. DOI:10.2529/PIERS061005101313



47. S. Liao and R. J. Vernon, The near-field and far-field properties of the cylindrical modal expansions with application in the image theorem, *2006 Joint 31st International Conference on Infrared Millimeter Waves and 14th International Conference on Terahertz Electronics*, Shanghai, 2006, pp. 260-260. DOI: 10.1109/ICIMW.2006.368468
48. S. Liao and R. J. Vernon, The cylindrical Taylor-interpolation FFT algorithm, *2006 Joint 31st International Conference on Infrared Millimeter Waves and 14th International Conference on Terahertz Electronics*, Shanghai, 2006, pp. 259-259. DOI: 10.1109/ICIMW.2006.368467
49. S. Liao and R. J. Vernon, On the image approximation for electromagnetic wave propagation and PEC scattering in cylindrical harmonics, *Progress In Electromagnetics Research*, Vol. 66, 65-88, 2006. DOI:10.2528/PIER06083002
50. S. Liao and R. J. Vernon, On fast computation of electromagnetic wave propagation through FFT, 2006 7th International Symposium on Antennas, Propagation & EM Theory, Guilin, 2006, pp. 1-4. DOI: 10.1109/ISAPE.2006.353495
51. S. Liao and R. J. Vernon, A new fast algorithm for field propagation between arbitrary smooth surfaces, *2005 Joint 30th International Conference on Infrared and Millimeter Waves and 13th International Conference on Terahertz Electronics*, Williamsburg, VA, USA, 2005, pp. 606-607 vol. DOI: 10.1109/ICIMW.2005.1572687
52. M. Hajizadegan, M. Sakhdari, S. Liao, and P.-Y. Chen, High-Sensitivity Wireless Displacement Sensing Enabled by PT-Symmetric Telemetry, *IEEE Transactions on Antennas and Propagation*, vol. 67, no. 5, pp. 3445-3449, May 2019, DOI: 10.1109/TAP.2019.2905892.
53. L. Zhu, N. Alkhaldi, H. M. Kadry, S. Liao, and P.-Y. Chen, A Compact Hybrid-Fed Microstrip Antenna for Harmonics-Based Radar and Sensor Systems, *IEEE Antennas and Wireless Propagation Letters*, vol. 17, no. 12, pp. 2444-2448, Dec. 2018, DOI: 10.1109/LAWP.2018.2877674.
54. S. Liao et al., Nuclear radiation induced atmospheric air breakdown in a spark gap, *IEEE Transactions on Plasma Science*, vol. 40, no. 4, pp. 990-994, Mar. 2012. DOI: 10.1109/TPS.2012.2187343
55. S. Liao et al., Microwave Remote Sensing of Ionized Air, *IEEE Geoscience and Remote Sensing Letters*, vol. 8, no. 4, pp. 617-620, Jul. 2011, DOI: 10.1109/LGRS.2010.2098016.

56. K. Wang, H. T. Chien, S. Liao, L. P. Yuan, S. H. Sheen, S. Bakhtiari and A. C. Raptis, Ultrasonic and electromagnetic sensors for downhole reservoir characterization, in *Proceedings of Thirty-Sixth Workshop on Geothermal Reservoir Engineering*, Stanford University, Stanford, California, January 31 - February 2, 2011 SGP-TR-191. arXiv:2007.00191: <https://arxiv.org/abs/2007.00191>
57. H. Soekmadji, S. Liao, and R. J. Vernon, Experiment and simulation on TE<sub>10</sub> cut-off reflection phase in gentle rectangular downtapers, *Letters of Progress in Electromagnetics Research*, vol. 12, pp. 79-85, 2009. DOI: 10.2528/PIERL09090707
58. H. Soekmadji, S. Liao, and R. J. Vernon, Trapped mode phenomena in a weakly overmoded waveguiding structure of rectangular cross section, *Journal of Electromagnetic Waves and Applications*, vol. 22, no. 1, pp. 143-157, 2008. DOI: 10.1163/156939308783122706
59. S. Liao and L. Ou, Bound States in Continuum and Zero-Index Metamaterials: A Review, *arXiv:2007.01361*, Jul. 2020. <https://arxiv.org/abs/2007.01361>
60. S. Liao, Optimal Feedback-Interferometric Fiber Laser Sensors, *2019 Photonics & Electromagnetics Research Symposium - Fall (PIERS - Fall)*, Xiamen, China, 2019, pp. 63-65. DOI: 10.1109/PIERS-Fall48861.2019.9021883
61. Y. Peng and S. Liao, On-chip ZIM-BiC Laser, in *2019 IEEE MTT-S International Conference on Numerical Electromagnetic and Multiphysics Modeling and Optimization (NEMO)*, 2019, pp. 1-4. DOI: 10.1109/NEMO.2019.8853827.
62. S. Liao, Spectral-domain MOM for Planar Meta-materials of Arbitrary Aperture Wave-guide Array, in *2019 IEEE MTT-S International Conference on Numerical Electromagnetic and Multiphysics Modeling and Optimization (NEMO)*, 2019, pp. 1-4, DOI: 10.1109/NEMO.2019.8853816.
63. Y. Zeng Z. Tang, S. Liao and Y. Peng, On-chip Coupler Using Zero-index Metamaterials, *2019 Photonics & Electromagnetics Research Symposium - Fall (PIERS - Fall)*, Xiamen, China, 2019, pp. 1458-1460. DOI: 10.1109/PIERS-Fall48861.2019.9021503
64. Y. Peng and S. Liao, ZIM Laser: Zero-Index-Materials Laser, *IEEE Journal on Multiscale and Multiphysics Computational Techniques*, vol. 4, pp. 133-142, 2019, DOI: 10.1109/JMMCT.2019.2905368.
65. S. Liao and L. Ou, High-Q Interstitial Square Coupled Microring Resonators Arrays, *IEEE Journal of Quantum Electronics*, 23

April 2020. DOI: 10.1109/JQE.2020.2989809

66. S. Liao, T. Wong, and L. Ou, Optimal feedback-interferometric fiber laser microphones, *Optics Letters, Optical Society of America (OSA)*, vol. 45, no. 2, pp. 423-426, Jan. 2020, DOI: 10.1364/OL.384225.
67. S. Liao and T. Wong, Optimal Design of Feedback-Interferometric Fiber Laser Sensors, *IEEE Sensors Journal*, vol. 19, no. 24, pp. 12016-12023, Dec. 2019, DOI: 10.1109/JSEN.2019.2936222.
68. S. Liao, T. Wong, Z. Wang, R. Wang, E. Clutter, and H.-T. Chien, Miniature fiber laser microphones with graphene diaphragms, *2018 IEEE Research and Applications of Photonics In Defense Conference (RAPID)*, Miramar Beach, FL, 2018, pp. 1-4. DOI: 10.1109/RAPID.2018.8508963
69. E. Clutter B. Matos, Z. Wang, R. Divan, A. Macrander and S. Liao, X-ray Writing of Optical Fiber Gratings with a nm-Mask, *The American Vacuum Society (AVS) Prairie Chapter*, The University of Chicago, IL USA, 2018. arXiv:2007.00683, <https://arxiv.org/abs/2007.00683>
70. S. Liao and A. Z. Genack, Polarization correlation in a quasi-1-D random system, in *Frontiers in Optics 2008/Laser Science XXIV/Plasmonics and Metamaterials/Optical Fabrication and Testing*, Rochester, New York, USA, 2008. DOI:10.1364/FIO.2008.FWV3
71. Stancil, D. D., "Kronig Penney model for periodically segmented waveguides," *Applied Optics, JOSA* , Vol. 35, No. 24, August 1996.